

Performance improvement speed control of IPMSM drive based on nonlinear current control

Muhammad USAMA^{id}, Jaehong KIM*^{id}

Department of Electrical Engineering, Chosun University, Gwangju, South Korea

Received: 22.06.2020

Accepted/Published Online: 08.12.2020

Final Version: 26.07.2021

Abstract: Recently model predictive control (MPC) scheme emerges as an efficient current control technique for dynamic performance of motor drives. For excellent dynamic performance, maximum torque per ampere (MTPA) control technique is utilized to achieve maximum torque while using minimum current constrain in contrast to conventional q-axis current control. Model predictive current control (MPCC) scheme alongside MTPA control is employed to replace the traditional constant gain proportional-integral (PI) current control and a nonlinear hysteresis current (HC) control schemes. The PI and hysteresis current controller offers satisfactory performance at ideal conditions but, with variable speed and load conditions, these control schemes cause high current harmonics, high torque ripples, and reduces the speed tracking performance. Therefore, MPCC is proposed to increase the performance of motor drive and reduces the current harmonics and torque ripple at varying load conditions. The proposed design is modeled in Matlab (MathWorks, Inc., Natick, MA, USA), and the results are compared with the traditional speed control schemes to verify the effectiveness. The simulation result shows that the MPCC for IPMSM offers high dynamic performance with reduced steady-state error under variable load conditions compared to conventional control scheme. With MPCC, the overall performance of IPMSM is improved and show robustness.

Key words: Interior permanent magnet synchronous motors, maximum torque per ampere, nonlinear control, speed control, torque response, stability analysis

1. Introduction

Recently, interior permanent magnet synchronous motor (IPMSM) drive has gained more attraction toward industrial applications. Because of various advantages, IPMSM motor drives have been used universally. High efficiency, less weight, small in size, low repairing cost, high power factor and torque to inertia ratio etc. make IPMSM the best choice for high-speed industrial applications [1, 2]. Some of the industrial drives such as servo motor need constant power operation. So, due to salient pole structure, IPMSM drive can be used in constant power application utilizing field weakening technique [3]. The direct control of motor field flux is not possible in IPMSM due to its structure, while the field can be weakened by demagnetizing the effect of d-axis motor current [4]. So, utilizing the benefit of field weakening approach, maximum torque is generated utilizing the minimum phase current [5] in contrast to q-axis current control. For IPMSM drive, due to saliency, maximum torque per ampere (MTPA) control technique is mostly employed because of its simple structure and gives efficient result.

With the improvement in power electronic technology, the rotor shaft speed control of IPMSM drive becomes simple and more efficient. Inverter with semiconductor switches (IGBT, MOSFET, etc) generates a

*Correspondence: Jaehong77@gmail.com

varying frequency from the direct voltage source which is then employed to IPMSM drive [6]. Several speed control techniques for PMSM drive were presented in researches based on linear and nonlinear current control schemes [7–11]. Lookup table is primarily used but they are very much dependent on motor parameters, and, due to parameter uncertainty, it cause the deviation from that efficient result. An online estimation model was proposed in [12]. But, as this approach doesn't depend on drive parameters and show the good performance against the parameter uncertainty, the algorithm might give erroneous result if the tracking speed of estimation design is slow. A signal injection method that injects the uncertainty to voltage or current was proposed in [13]. However, it results in additional losses and cause harmonic distortion, which affects the comprehensive performance of motor drive.

In variable frequency drives, the closed-loop control of motor requires fast and efficient information of the rotor shaft speed and position. The precision with which motor drives follows the reference speed command is significant performance parameter [14], the traditional control technique utilized the PI controller to regulate the shaft speed and motor phase current. As for efficient performance, the proportional-integral (PI) gain value needs to be accurate, and gain values are selected in such a way that the closed-loop bandwidth is larger than the speed bandwidth [15]. To increase the dynamic performance of the motor drive, several predictive control techniques are studied in literature [16, 17]. Conventional predictive control such as HC control maintains the control variables within the hysteresis band, and, for efficient drive response, the hysteresis band need to be small, which will cause high switching losses and affect the inverter [18]. Thus, HC control is restricted to low power applications. The model predictive control (MPC) technique is proposed as it can handle nonlinearities of multiple output and input of plant and execute them in a unified manner. MPC consists of three main parts: a model of the system, a predictive algorithm, and a cost function. MPC helps to eliminate the modulation block from control design and is well suited for online optimization [19, 20]. The two main groups of MPC are finite control set MPC (FCS-MPC) and continuous control set MPC (CCS-MPC). CCS-MPC employs the average model of the system; it has complex optimization process and work with large sample time that will affect the performance when the system delay is taken into account. By contrast, FCS-MPC employs the internal model of the system and work with small sampling time, and this makes it versatile for high performance applications. FCS-MPC is categorized in two groups: optimal switching vector MPC that computes the predictive values for voltage source inverter (VSI) through searching algorithm, and only one VV is utilized in whole switching period where as optimal switching sequence MPC overcomes this drawback and generates limited number of possible inverter switching state for the entire period [21, 22]. In general, MPC is time consuming and cost computational power of microprocessor. Therefore, in designing MPC, the important factors are reduction of computational cost, predictive horizon extension, and selection of cost function [23, 24].

The objective of this paper is to present the steady-state and robust dynamic performance of IPMSM drive under the variable load conditions. Salient pole structure and the capability of utilizing maximum torque using minimum current values make IPMSM an excellent candidate for high speed applications. MPCC considering MTPA is proposed for IPMSM to determine optimal voltage vectors regardless of optimal switching sequence, which helps to minimize torque ripple and harmonic distortion that tends to increase the overall efficiency of the motor drive. The current controller is designed based on finite control set MPC technique with reduced computational load. FSC-MPCC employs the discrete-time internal model of the motor drive to predict the future state over a discrete sample time. Phase voltages are obtained based on inverter switching states. The optimal voltage vector across the motor drive is selected based on the control objective defined by a cost function. In contrast to conventional closed-loop speed control, the intended design is simple, intuitive, easy to implement,

shows robustness, handles the nonlinearities of motor drive, and reduces the steady-state errors. The results of proposed method are compared with traditional methods, and overall performance of motor drive is notably improved with designed MPCC.

This paper is organized as follows: mathematical modeling and MTPA control technique for IPMSM drive is described in Section 2. The proposed speed control model is developed in Section 3. Simulation results and comparison with traditional control scheme are shown in Section 4 to verify the efficiency and robustness. Finally, the conclusion is given in Section 5.

2. Mathematical model of IPMSM

VSI connected to IPMSM controlled by a predictive technique is depicted in Figure 1. Dc voltage source is the input to voltage source inverter (VSI) and insulated-gate bipolar transistor (IGBT) switches, which provides the voltage across the motor phase winding based on switching signal provided by the model predictive control (MPC). The MTPA control approach is constructed to operate with the dynamic model of IPMSM in the rotor dq reference frame. Eddy current, hysteresis losses, and saturation effect are not considered in this well-known model. In the three-phase coordinate system, the voltage equation of IPMSM is derived as in [25]:

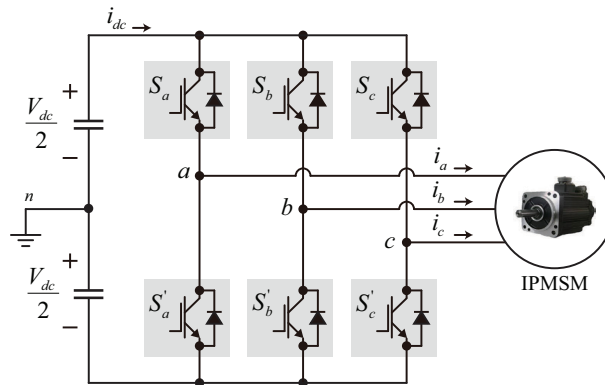


Figure 1. Power circuit topology of 2-level VSI-fed IPMSM drive system.

$$\begin{bmatrix} v_a \\ v_b \\ v_c \end{bmatrix} = r_s \begin{bmatrix} i_a \\ i_b \\ i_c \end{bmatrix} + \frac{d}{dt} \begin{bmatrix} \lambda_a \\ \lambda_b \\ \lambda_c \end{bmatrix}, \tag{1}$$

where v_{abc} , i_{abc} , r_s , and λ_{abc} shows the drive phase voltage, drive phase current, stator winding resistance, and flux linkage in stator windings, respectively. The dq transformation is employed to transform (1) into exciting frame. The dq model of IPMSM is derived as:

$$\begin{bmatrix} v_d^e \\ v_q^e \end{bmatrix} = \begin{bmatrix} r_s + L_d p & -\omega_r L_q \\ \omega_r L_d & r_s + L_q p \end{bmatrix} \begin{bmatrix} i_d^e \\ i_q^e \end{bmatrix} + \begin{bmatrix} 0 \\ \omega_r \lambda_m \end{bmatrix}. \tag{2}$$

where ω_r and λ_m are the rotor speed and flux linkage due to rotor side permanent magnet. L_d and L_q are the d-axis and q-axis inductance. Equation (1)-(2) represent the mathematical model of IPMSM. Due to

the salient pole structure of IPMSM drive, electromagnetic torque equation is derived as:

$$T_e = \frac{3P}{2}[\lambda_m i_q^e + (L_d - L_q)i_d^e i_q^e]. \quad (3)$$

where P and T_e are pole pairs and electromagnetic torque, respectively. The generated torque in (3) depends on reluctance torque and magnetic torque. Magnetic torque, $\lambda_m i_q^e$, describes the torque component owing to rotor permanent magnet flux, and the reluctance torque, $(L_d - L_q)i_d^e i_q^e$, describes the torque component owing to the product of dq-axis inductance difference and current. The mechanical model of IPMSM is given as:

$$T_e = T_L + B\omega_m + Jp\omega_m, \quad (4)$$

where B is the damping coefficient, J is the rotor inertia, ω_m and T_L are the mechanical shaft speed and load torque, respectively.

In IPMSM drives, due to salient pole structure, MTPA control can't be attained by simply utilizing q-axis current controller because, if $i_d = 0$, then the magnitude of the terminal voltage increase as the speed increases, and the saturation of current regulator occurs at high speed for given torque, which may cause the instability of drive. When we use $i_d = 0$, the control of interior PMSM is simplified, making electromagnetic torque linear to q-axis current, which means reluctance torque of the motor is not used. This causes error during the control of IPMSM because the maximum capacity of the motor drives to generate the torque is not utilized under different operating conditions [26]. If the magnitude of the phase current is fixed, then the dq-axis current will be the point on a circle as depicted in Figure 2a. The MTPA curve is shown as the phase current magnitude increases from 0 to the maximum value. The torque curve intersects the current circle tangentially. So, by polar description, the dq-axis current can be obtained as [1]:

$$i_d^e = -I_s \sin \beta. \quad (5)$$

$$i_q^e = I_s \cos \beta. \quad (6)$$

where the current angle β is given as:

$$\beta = -\tan^{-1} \frac{i_d^e}{i_q^e}. \quad (7)$$

$$T_e = \frac{3P}{2}[\lambda_m I_s \cos \beta - (L_q - L_d)2I_s^2 \cos \beta \sin \beta]. \quad (8)$$

So, by putting (5-6) in (3), we will get the torque in terms of current angle. Based on (8), the angle versus torque response is depicted in Figure 2b as the sum of magnetic and reluctance torque. Peak torque is obtained when the q-axis inductance is greater than d-axis and a current angle greater than 0.

To establish MTPA control technique, q-axis current is utilized to obtain d-axis current by differentiating (8) with respect to current angle (β) and setting it to zero [27]. With the help of reluctance torque in IPMSM drives, the performance of IPMSM increases in wide speed range and increase the efficiency of control.

$$\frac{dT_e}{d\beta} = \frac{3P}{2}[-\lambda_m I_s \sin \beta + \frac{(L_q - L_d)}{2} I_s^2 \cos 2\beta] = 0. \quad (9)$$

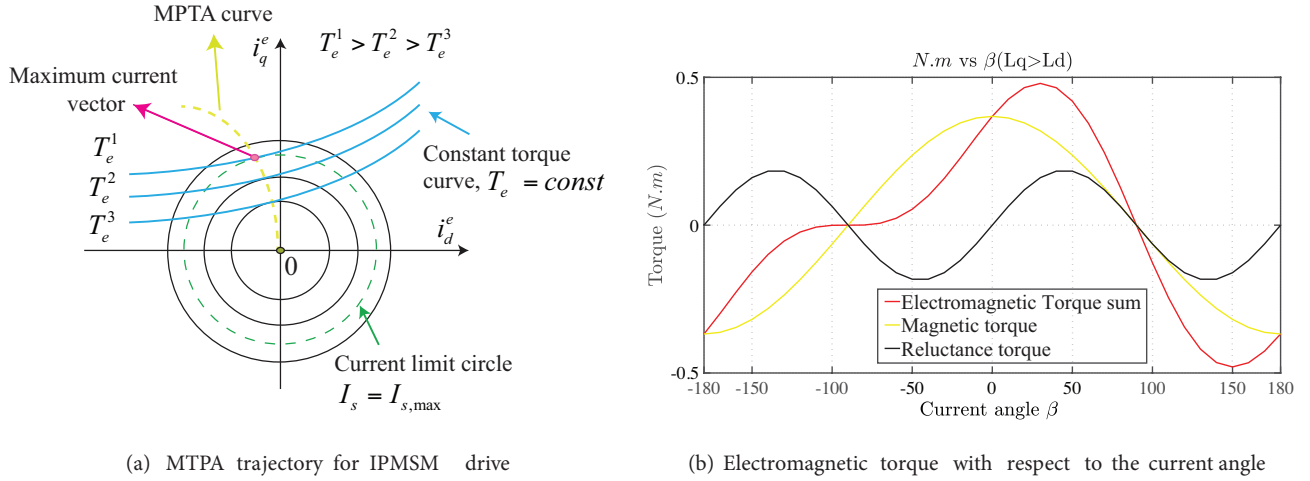


Figure 2. MTPA trajectory and electromagnetic torque characteristic of IPMSM.

$$\beta = \sin^{-1} \left[\frac{-\lambda_m + \sqrt{\lambda_m^2 + 8[L_q - L_d]^2 I_s^2}}{4[L_q - L_d]I_s} \right]. \quad (10)$$

where

$$I_s = \sqrt{i_d^2 + i_q^2},$$

by substituting (10) in (5) we will get d-axis reference current as

$$i_d^* = \frac{\lambda_m - \sqrt{\lambda_m^2 + 8[L_q - L_d]^2 I_s^2}}{4[L_q - L_d]}. \quad (11)$$

For simplification, the dq-axis currents are expanded using Taylor series expansion [28]. The effect of higher-order is minimum in the Taylor series expansion, so the d-axis reference current equation is derived as:

$$i_d^* = \frac{[L_d - L_q]}{\lambda_m} i_q^{*2}, \quad (12)$$

and

$$i_q = \text{sgn}(I_s) \sqrt{I_s^2 - i_d^{*2}}, \quad (13)$$

where

$$\text{sgn}(I_s) = \text{if} \begin{cases} I_s \geq 0, & 1. \\ \text{otherwise,} & -1. \end{cases}$$

The MTPA control approach utilized the minimum current to provide the maximum torque, which helps to reduce the copper loss and increase the overall efficiency of the control system. Moreover, the MTPA control approach is simple to design and easy to implement and show excellent dynamic performance at wide speed under variable load conditions.

3. Closed loop speed control

3.1. Conventional closed loop speed control

In the conventional vector controls scheme, the PI and HC controllers are widely employed to generate the pulse order for switching the VSI. In PI current control scheme, PWM method is utilized to shape the output voltage across inverter. Among different modulation techniques, the space vector pulse width modulation (SVPWM) technique is widely used because it provides 15 % raise in dc-voltage utilization. On the other hand, in HC control method, the actual and the reference current are compared in hysteresis comparator, and the modulation block is eliminated and the switching pulse order is guaranteed based on each hysteresis comparator such that phase current are compelled to remain within hysteresis band. The traditional PI linear control scheme is operating on a fixed frequency, but is highly sensitive to parameter variation and load disturbance; whereas, nonlinear HC control operates on variable frequency and is highly dependent on hysteresis band. For an excellent dynamic performance, the constant PI gain values need to be exact and are attained in such a way that the closed-loop bandwidth is larger than the speed bandwidth, while, for nonlinear HC control, the high dynamic performance of motor drive can be attained by utilizing small hysteresis band that will affect inverter and cause high switching losses. So, to overcome these issue, the model predictive current control technique is proposed.

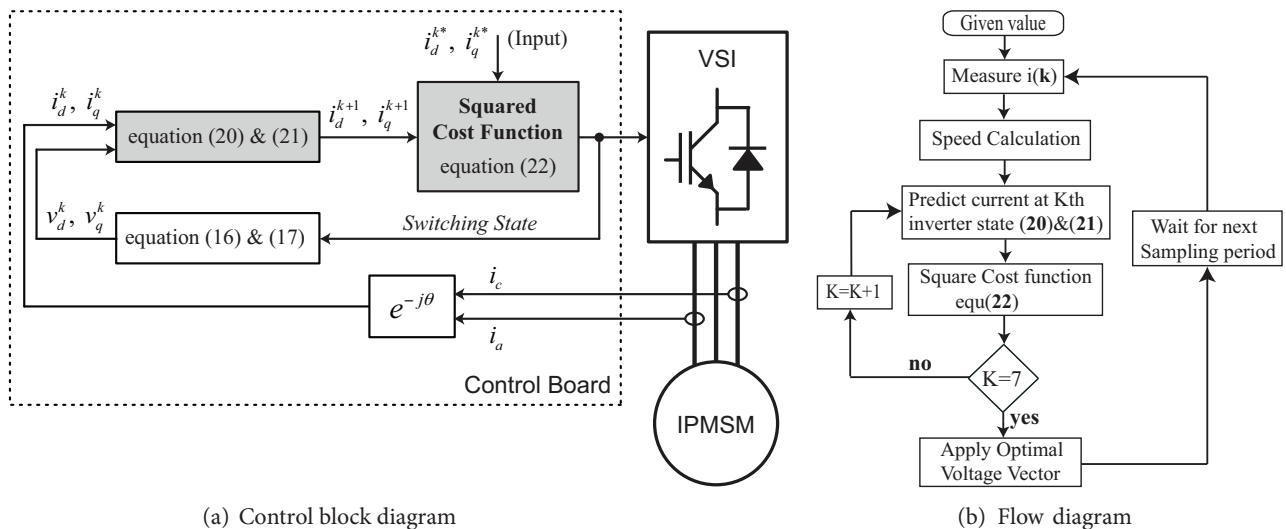


Figure 3. System architecture of the proposed MPCC.

3.2. Proposed closed loop speed control

In this section, the proposed speed control model is discussed in detail. First, the discrete-time model of the IPMSM is specified. Then, the FCS-MPCC is considered, which generates the pulse order for the VSI to control the reference model of the design.

MPC approach utilizes the discrete-time model of the system to predict the future value of load phase current for each possible VV. An internal discrete-time model of the IPMSM drive was employed to predict the future state of the output state variable that is used to control the state input over the sample time T_s . Utilizing the forward Euler approximation is computationally cheap and will not rise the computational burden

of MPC [29–32]. Thus, the discrete-time model of the IPMSM drive is obtained:

$$\frac{di}{dt} \approx \frac{[i^{k+1} - i^k]}{T_s}. \quad (14)$$

VSI model is checked by the control design to attain the optimal output voltage vector(VV). Table 1 shows the state of VSI switches [33]. The VSI is modelled as:

$$S = \frac{2}{3}(S_a + e^{j\frac{2\pi}{3}} S_b + e^{j\frac{4\pi}{3}} S_c). \quad (15)$$

Table 1. Inverter switching configurations and voltage vectors.

Inverter on legs	Voltage vector	Switching states		
S	n	Sa	Sb	Sc
$S_a^i S_b^i S_c^i$	$v_0=0$	0	0	0
$S_a^i S_b^i S_c^i$	$v_1=\frac{2}{3}V_{dc}e^{j\frac{4\pi}{3}}$	0	0	1
$S_a^i S_b^i S_c^i$	$v_2=\frac{2}{3}V_{dc}e^{j\frac{2\pi}{3}}$	0	1	0
$S_a^i S_b^i S_c^i$	$v_3=\frac{2}{3}V_{dc}e^{j\pi}$	0	1	1
$S_a^i S_b^i S_c^i$	$v_4=\frac{2}{3}V_{dc}$	1	0	0
$S_a^i S_b^i S_c^i$	$v_5=\frac{2}{3}V_{dc}e^{j\frac{5\pi}{3}}$	1	0	1
$S_a^i S_b^i S_c^i$	$v_6=\frac{2}{3}V_{dc}e^{j\frac{\pi}{3}}$	1	1	0
$S_a^i S_b^i S_c^i$	$v_7=0$	1	1	1

The drive phase voltages determined by the switching states of VSI are given as follows [34]:

$$\begin{bmatrix} v_{as} \\ v_{bs} \\ v_{cs} \end{bmatrix} = \frac{V_{dc}}{3} \begin{bmatrix} 2 & -1 & -1 \\ -1 & 2 & -1 \\ -1 & -1 & 2 \end{bmatrix} \begin{bmatrix} S_a \\ S_b \\ S_c \end{bmatrix}, \quad (16)$$

With the possible combinations of switching patterns, the phase voltages are attained. Thus, by utilizing the Park's transformation, dq-voltage is formed and given as:

$$\begin{bmatrix} v_d^e \\ v_q^e \\ v_0^e \end{bmatrix} = \frac{2}{3} \begin{bmatrix} \cos\theta & \cos(\theta - \frac{2\pi}{3}) & \cos(\theta + \frac{2\pi}{3}) \\ -\sin\theta & -\sin(\theta - \frac{2\pi}{3}) & -\sin(\theta + \frac{2\pi}{3}) \\ \frac{1}{\sqrt{2}} & \frac{1}{\sqrt{2}} & \frac{1}{\sqrt{2}} \end{bmatrix} \begin{bmatrix} v_{as} \\ v_{bs} \\ v_{cs} \end{bmatrix}. \quad (17)$$

By Euler forward approximation, (2) can be shown in the discrete-time model as

$$v_d^k = r_s i_d^k + \frac{L_d}{T_s}(i_d^{k+1} - i_d^k) - \omega_r^k L_q i_q^k, \quad (18)$$

$$v_q^k = r_s i_q^k + \frac{L_q}{T_s}(i_q^{k+1} - i_q^k) + \omega_r^k L_d i_d^k + \omega_r^k \lambda_m. \quad (19)$$

Therefore, the discrete-time current model of the drive is derived by utilizing (18) and (19), and expressed as:

$$i_d^{k+1} = [(1 - \frac{T_s r_s}{L_d})i_d^k + \frac{T_s}{L_d}(\omega_r^k L_q i_q^k + v_d^k)], \quad (20)$$

$$i_q^{k+1} = \left[\left(1 - \frac{T_s r_s}{L_q} \right) i_q^k + \frac{T_s}{L_q} (v_q^k - \omega_r^k L_d i_d^k - \omega_r^k \lambda_m) \right], \quad (21)$$

where i_{dq}^k are the measured output state variables at K^{th} sampling instant; i_{dq}^{k+1} are the predictive output state variables at the $k + 1$ sampling time period; and v_{dq}^k are the control input state variables that must be selected based on the inverter switching state. The motor speed is considered constant at several control instances as the electromechanical time constant of the motor drive is lower than the mechanical time constant, which shows $\omega_r^{k+1} \approx \omega_r^k$ [35]. As ω_r^k is the function of input control variable v_{dq}^k , the system is a nonlinear system. The possibility of rotor shaft speed ω_r^k for a given reference, state variables i_{dq}^{*k} will be determined based on input control variables v_{dq}^k with availability of optimal output voltage vector.

The design of FCS-MPCC for the IPMSM drive is shown in Figure 3a. To obtain optimal VV, the selection of cost function is essential. In the current control mechanism, the inverter keeps the most important consideration of keep tracking the reference currents to measure current accurately. The flow diagram for the proposed design is demonstrated in Figure 3b. As i_{dq}^k are directly controlled in FCS-MPCC, the square cost function is selected as

$$h = (i_d^{*k} - i_d^{k+1})^2 + (i_q^{*k} - i_q^{k+1})^2. \quad (22)$$

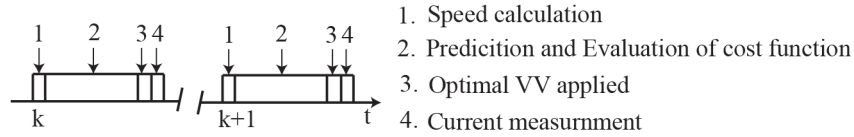


Figure 4. Time obtained by different task [31].

The square cost function in the proposed MPCC guarantees the least number of switches change in the steady-state; whereas, the control error is subjected to reduce the transient period to verify the stability of the system. With the help of MTPA technique, i_{dq}^{*k} reference current values are obtained. The switching states in Table 1 were applied across the inverter, which caused the applied motor phase current to attain the current reference value in the next sample time period after the cost function is minimized. As a result, the predictive currents were utilized across the drive and operated according to the current reference value. The control method of the given MPCC has two main parts. First, it determines the optimal output VV that yields the lowest cost index. Second, it defines the duration of output VV in the next control period to minimize the cost index. In given VSI, there are eight switching patterns with VVs $\mathbf{V}_0, \mathbf{V}_1, \dots, \mathbf{V}_7$, as given in Table 1. For the selection of optimal VVs, the motor phase voltage is calculated based on (16) and predicts the future current values based on (20-21) for all voltage vector that VSI can generate. As the input control variable v_{dq}^k depends on the rotor speed as given in (18-19), the discrete state-space model of IPMSM becomes nonlinear. From encoder, the rotor shaft speed is calculated and is given to MPCC block. From Table 1, the possibility of input variable \mathbf{V}_{dq}^k can be obtained in terms of the inverter input voltage. Once the optimal output VV is selected, the pulse order for insulated-gate bipolar transistor (IGBT) switches of VSI is generated. Time frame for different task is depicted in Figure 4 which describes that the inverter switching states that are applied at

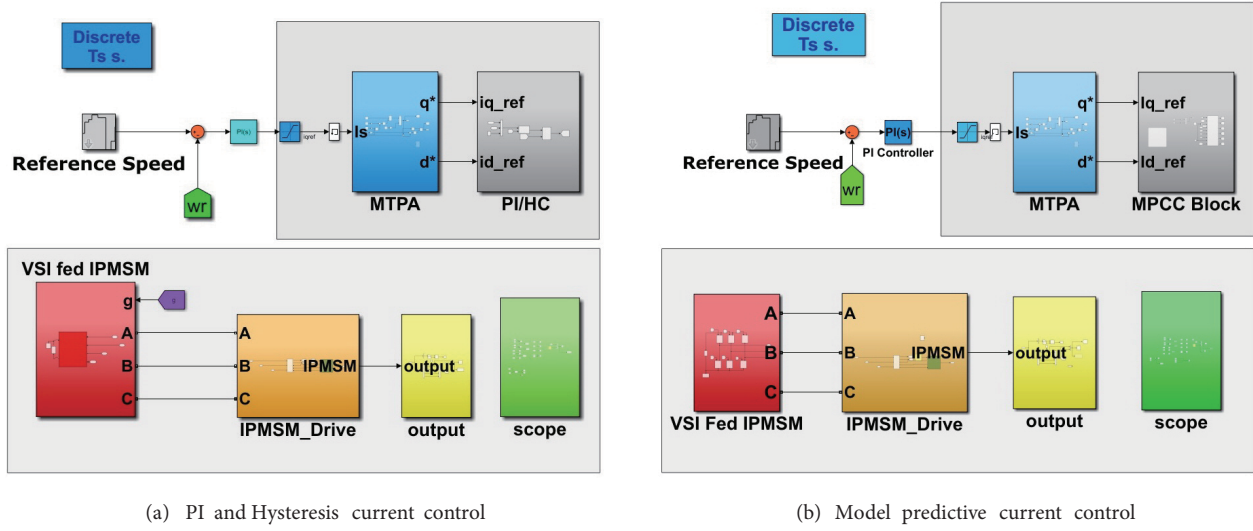


Figure 5. Simulink models to compare the speed control performance of IPMSM with respect to different current control methods.

$K + 1$ interval are obtained in K time period. Because of the motor, nonlinear model and the evaluation of cost function the predictive model consume a lot of time to attain optimal voltage vector that need to determine inverter switching sequence. The advantage of selecting the small sample time helps to reduce torque ripples and current harmonic distortion that tends to increase the efficiency of the drive. The simulation model of the proposed design is demonstrated in Figure 5b. The performance of the IPMSM drive is improved with the proposed design and is discussed in the next section.

3.2.1. Stability analysis

For stability analysis of the proposed system, let a positive real function, V^k , as

$$V^k \equiv |e_d^k|^2 + |e_q^k|^2, \quad (23)$$

where $e_d^k = i_d^{*k} - i_d^k$ and $e_q^k = i_q^{*k} - i_q^k$. With a sufficiently large sampling frequency in the steady-state, the current reference can be fixed, i.e., $i_d^{*k+1} = i_d^{*k}$. So d -axis current error at $(k + 1)$ -th sampling instant is calculated from (20) as

$$e_d^{k+1} = i_d^{*k} - i_d^{k+1} = e_d^k + \underbrace{\frac{T_s}{L_d} (r_s i_d^k - \omega_r^k L_q i_q^k - v_d^k)}_{u_d^k}.$$

Then, it is obvious from Minkowski's inequality that

$$|e_d^{k+1}|^2 = |e_d^k + u_d^k|^2 \leq |e_d^k|^2 + |u_d^k|^2,$$

for all u_d^k values. By substituting u_d^k to (18), we get $u_d^k = i_d^k - i_d^{k+1}$. And the volt-second balance condition at the stator inductance, L_d , during the steady-state implies that $i_d^k - i_d^{k+1} = 0$. Therefore, the

following inequality holds:

$$|e_d^{k+1}|^2 - |e_d^k|^2 \leq 0. \tag{24}$$

Monotonic decrease of $|e_d^k|^2$ is achieved with this negative squared error difference.

On the other hand, the q -axis current error, e_q^{k+1} , is calculated from (21) with a fixed current reference as

$$e_q^{k+1} = i_q^{*k} - i_q^{k+1} = e_q^k + \underbrace{\frac{T_s}{L_q} (r_s i_q^k + \omega_r^k L_d i_d^k + \omega_r^k \lambda_m - v_q^k)}_{u_q^k}.$$

In the same way as above, it can be easily proven that

$$|e_q^{k+1}|^2 - |e_q^k|^2 \leq 0. \tag{25}$$

So $|e_q^k|^2$ is also monotonically decreasing. As a result, (23), which is the same form as the proposed cost function, is monotonically decreasing over time and thus, the proposed system is asymptotically stable. Stability of the proposed system is also examined through the simulation studies.

4. Results and discussion

The simulation models of the control schemes are depicted in Figure 5. In the conventional model, the PI and hysteresis control schemes are simulated as shown in Figure 5a; whereas, in Figure 5b, the proposed MPC is modelled. The system parameters are given in Table 2. The simulation results for the proposed and conventional schemes are presented to evaluate the control behaviour at different reference speed under varied load conditions. Figure 6 shows the rotor shaft speed tracking the reference speed under the load condition. The reference speed is 500 rpm under the load torque of 3 Nm, increasing to 800 rpm at 0.5 s. The load torque increases from 3 Nm to 7 Nm at 0.7 s. The steady-state error and speed tracking performance of motor drive operated by MPCC is outstanding as compared to conventional control schemes.

Table 2. Control parameters of utilized IPMSM.

Parameters	Value
Sample time period (μs)	1
DC voltage (V)	600
Stator resistance (Ω)	2.5
Poles pairs (P)	3
d-axis inductance (mH)	15.025
q-axis inductance (mH)	30.175
Moment of inertia ($kg.m^2$)	0.00365
Flux (mWb)	0.5283
Damping coefficient	0.0011

Similarly the motor phase current and the harmonic order is shown in Figure 7 and Figure 8. The proposed design shows a good response in reducing ripples and harmonic distortion at a wide speed operation

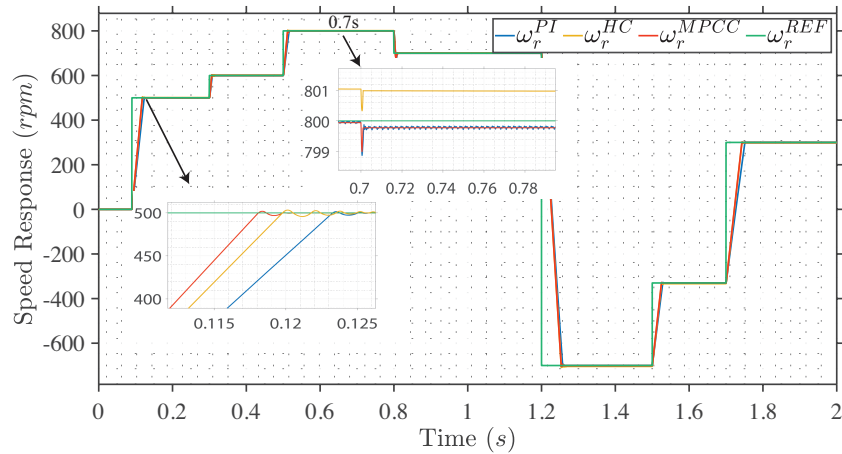


Figure 6. Simulation test results of reference and actual rotor shaft speed for various operation range under different control schemes.

range. MTPA control technique is employed to maximize the torque utilization with minimum current value; the dq-axis currents are depicted in Figure 9 and Figure 10. By comparing both results, it can be observed that the conventional control scheme has considerable high current ripple during both steady-state and dynamic state. Figure 11 demonstrates the torque response of the motor drive. The ripples across the torque are reduced with fast convergence rate. The result shows that the proposed control model is robust, and it shows excellent dynamic performance. The testing is also done under the varying step load and is depicted in Figure 12 and Figure 13. Initially no load is applied, then 0.4 s the 5 Nm load torque is applied, and the drive response is examined; the load torque gradually increased to 20 Nm at 1.1 s, and the drive response is shown.

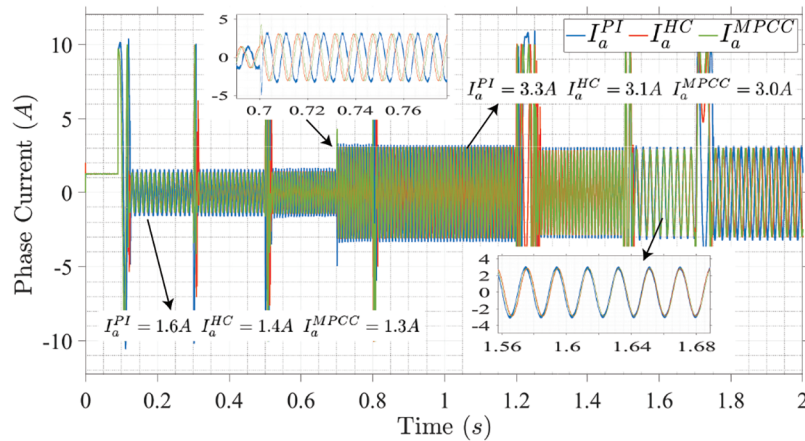


Figure 7. Three-phase measured current for operation of IPMSM drive based on conventional and proposed current control: pi current control, hysteresis current control, and model predictive current control.

At 1.4 s the load torque is reduced to 10 Nm and the tracking performance is observed. At last, 5 Nm load is applied at 1.75 s. The result shows that the speed and torque convergence rate to the reference value is fast and excellent in proposed design as compared to conventional control method. The motor phase current response of the proposed model is significant with designed MPCC. Figure 14 shows more specific

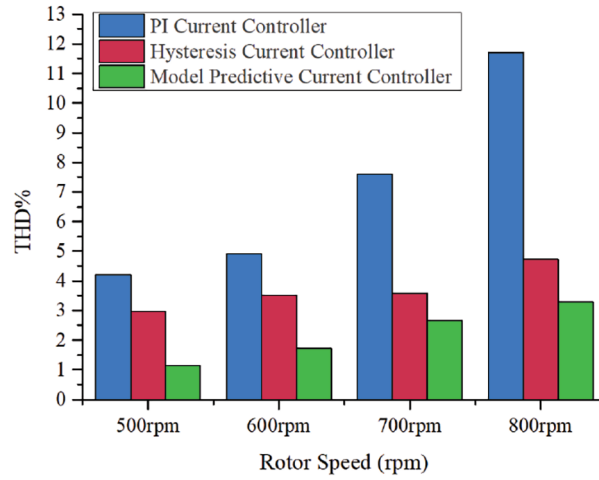


Figure 8. Total harmonic distortion for the measured current of IPMSM drive based on linear and nonlinear control scheme.

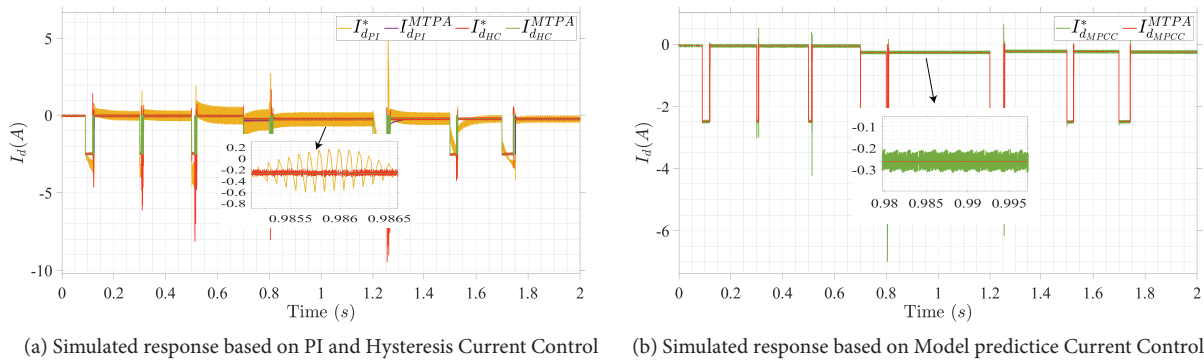


Figure 9. Stator d-axis current reference and its response.

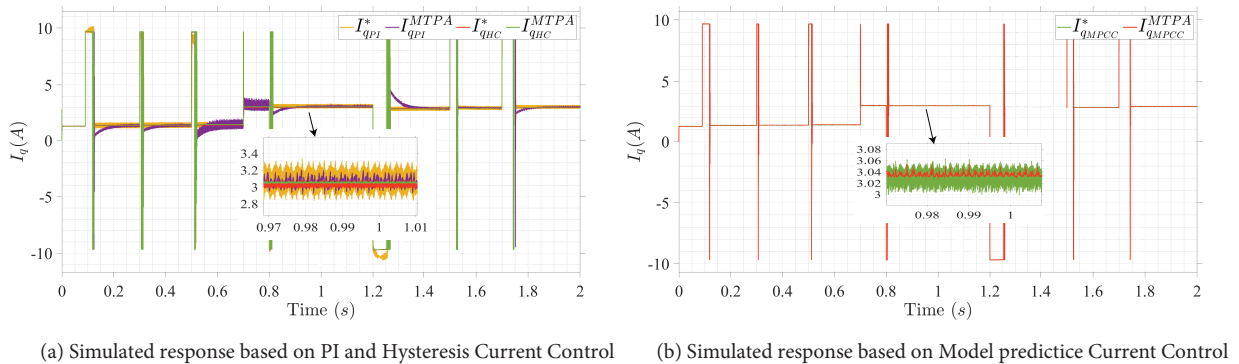


Figure 10. Stator q-axis current reference and its response.

information regarding speed response, torque ripple, and maximum drive phase current. Table 3 is constructed utilizing the variable load at dynamic and steady state to summarize the analysis of proposed and conventional

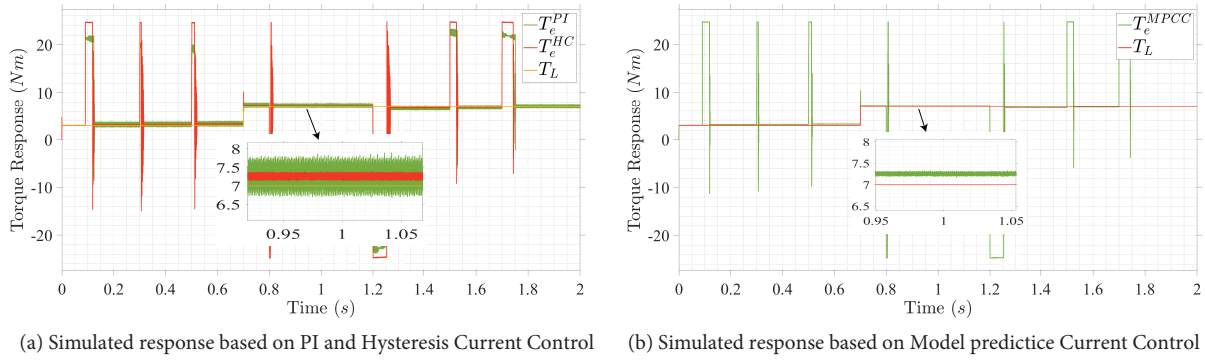


Figure 11. Electromagnetic torque response for speed reference steps.

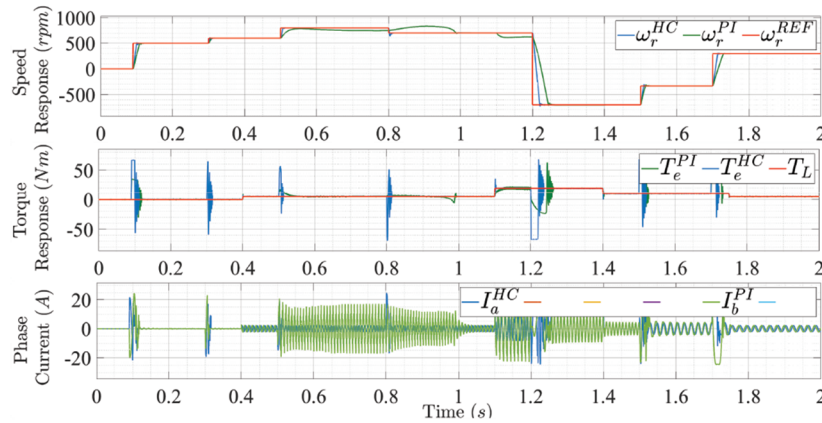


Figure 12. Rotor speed, electromagnetic torque and stator current response under variable load conditions, and reverse speed using conventional control scheme.

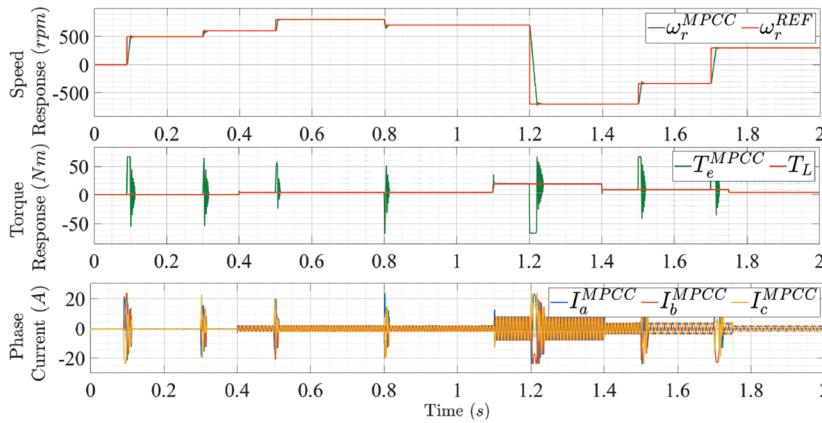


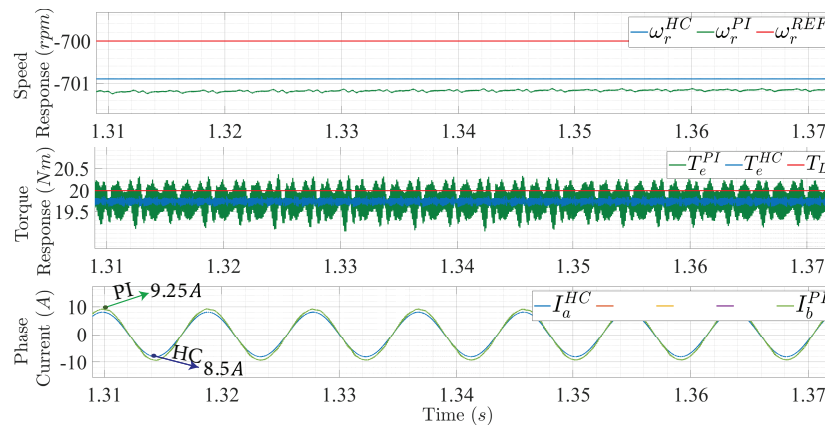
Figure 13. Rotor speed, electromagnetic torque and stator current response under variable load conditions, and reverse speed using proposed control scheme.

control schemes. To evaluate the stability performance of proposed design, the most common method is utilized by running multiple simulation tests under parameter variation to check how VSI respond based on model

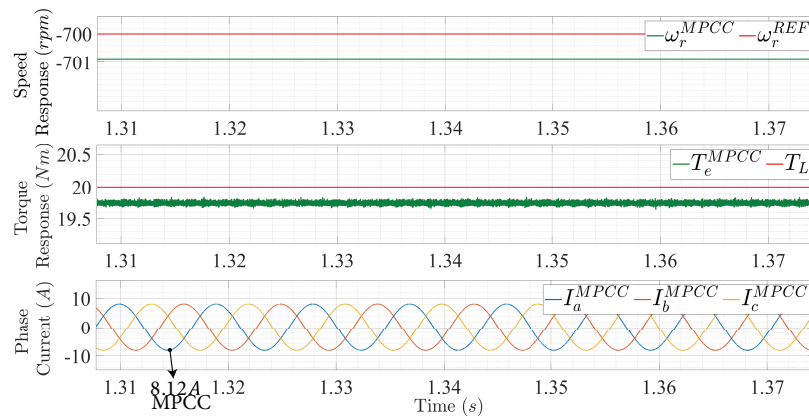
parameter variations. Figure 15 shows the stability performance of the designed MPCC. The convergence rate for the speed, torque, and phase current is fast verifying that the proposed control design is effective for wide speed range of IPMSM.

Table 3. Comparative system performance analysis by employing linear and nonlinear control scheme.

Parameters	PI	HC	MPCC
Speed tracking	Average	Good	Excellent
Speed Steady-state Error	Moderate	Minimum	Minimum
Speed response time($\omega_r^{max}/\omega_r^{min}$)	27ms/38ms	20ms/27ms	15ms/22ms
Torque Response	Slow	Medium	Fast
Torque Ripple	Higher	Moderate	Lower
Switching Frequency	Fixed	Variable	Variable
Current Harmonics	Higher	Moderate	Lower
Control Efficiency	Average	Good	Excellent

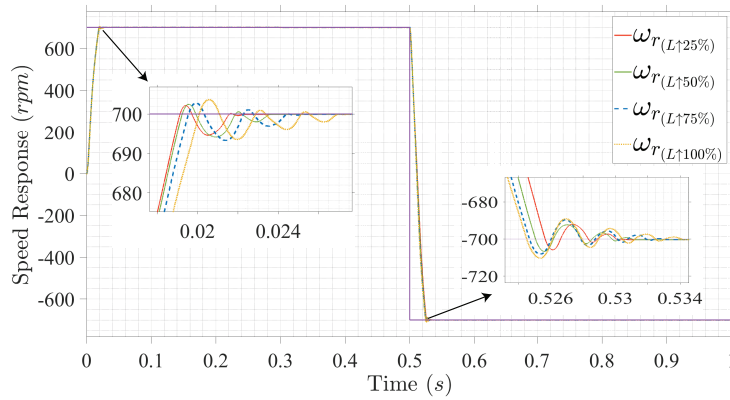


(a) Conventional control scheme

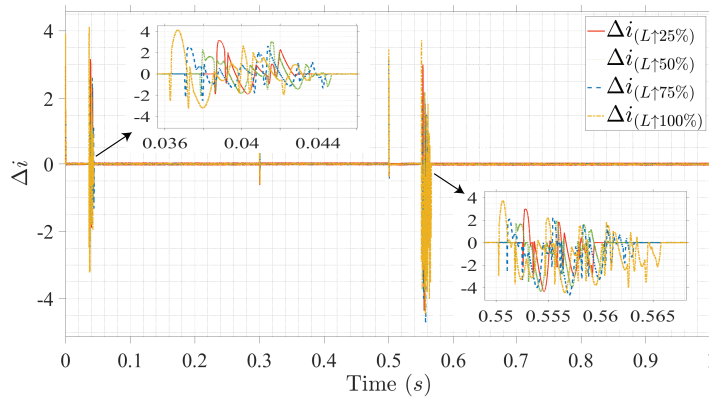


(b) Proposed control scheme

Figure 14. Motor response at negative shaft speed and maximum load torque (zoomed).



(a) Speed overshoot and tracking performance under parameter variation



(b) Current tracking error under parameter variation

Figure 15. Stability performance of proposed non-cascaded control scheme under variation in the stator inductance of IPMSM drive.

5. Conclusion

The paper presents an efficient speed control technique for excellent dynamic performance of IPMSM drive. The proposed design eliminates the modulation block and utilized minimum current constrain to achieve maximum torque in contrast to conventional control schemes. The MPCC algorithm is employed for logical firing of power electronic switches. With optimize control algorithm , the speed response of motor drive becomes fast and robust under the varying load conditions. The steady-state error across the output of the motor drive is reduced tremendously with the quick dynamic response. With designed MPCC, the overall response of the IPMSM drive is enhanced. The validity of the control model is confirmed by Matlab/Simulink (MathWorks, Inc.) work-space 2019b. The result verifies the robustness and effectiveness of designed MPCC. Compared with the traditional control schemes, the current harmonics and torque ripple across the proposed design is minimal with excellent drive performance. This control scheme will be effective for the study of sensorless speed control of IPMSM drive.

Acknowledgment

This work was supported by the Technology Innovation Program (20007237, Demonstration of Domestically Developed CNC Systems for Machine Tools) funded by the Ministry of Trade, Industry and Energy (MI, Korea).

References

- [1] Nam K. Permanent magnet AC motors. In: Handbook of AC motor control and electric vehicle applications, New York: CRC Press, 2010, pp. 167-191.
- [2] Lei M, Sanada M, Morimoto S, Takeda Y. Advantages of IPMSM with adjustable PM armature flux linkage in efficiency improvement and operating range extension. Proceedings of the Power Conversion Conference-Osaka 2002 (Cat. No.02TH8579), Osaka, Japan 2002; 1: 136-141. doi: 10.1109/PCC.2002.998536
- [3] Uddin MH, Radwan TS, Rahman MA. Performance of interior permanent magnet motor drive over wide speed range. IEEE Transactions on Energy Conversion 2002; 17(1): 79-84. doi: 10.1109/60.986441
- [4] Sneyers B, Novotny DW, Lipo T. A. Field-weakening in buried permanent magnet AC motor drives. IEEE Transactions on Industry Applications 1985; IA-21: 398-407. doi: 10.1109/TIA.1985.349661.
- [5] Halder S, Agarwal P, Srivastava SP. Comparative analysis of MTPA and ZDAC control in PMSM drive. Annual IEEE India Conference (INDICON), New Delhi; 2015. pp. 1-5. doi: 10.1109/INDICON.2015.7443809
- [6] Castellani S, Sulligoi G, Tassarolo A. Comparative performance analysis of VSI and CSI supply solutions for high power multi-phase synchronous motor drives. 2008 International Symposium on Power Electronics, Electrical Drives, Automation and Motion, Ischia; 2008. pp. 854-859. doi: 10.1109/SPEEDHAM.2008.4581250
- [7] Rebeiro RS, Uddin MH. Performance analysis of an FLC-based online adaptation of both hysteresis and PI controllers for IPMSM drive. IEEE Transactions on Industry Applications 2012; 48 (1): 12-19. doi: 10.1109/TIA.2011.2175876
- [8] Huang W, Zhang Y, Zhang X, Sun G. Accurate torque control of interior permanent magnet synchronous machine. IEEE Transactions on Energy Conversion 2014; 29 (1): 29-37. doi: 10.1109/TEC.2013.2290868
- [9] Ogbuka C, Nwosu C, Agu M. A high performance hysteresis current control of a permanent magnet synchronous motor drive. Turkish Journal of Electrical Engineering and Computer Sciences 2017; 25: 1-14. doi: 10.3906/elk-1505-160
- [10] Butt C, Hoque MA, Rahman MA M. Simplified fuzzy-logic-based MTPA speed control of IPMSM Drive. IEEE Transactions on Industry Applications 2004; 40 (6): 1529-1535. doi: 10.1109/TIA.2004.836312
- [11] Nalepa R, Orłowska-Kowalska, T. Optimum trajectory control of the current vector of a nonsalient-pole PMSM in the field-weakening region. IEEE Transactions on Industrial Electronics 2012; 59: 2867-2876.
- [12] Morimoto S, Sanada, M, Takeda, Y. Wide-speed operation of interior permanent magnet synchronous motors with high-performance current regulator. IEEE Transactions on Industry Applications 1994; 30: 920-926. doi: 10.1109/28.297908.
- [13] Kim S, Yoon Y, Sul S, Ide K. Maximum torque per armature (MPTA) control of an IPM machine based on signal injection considering inductance saturation. IEEE Transactions on Power Electronics 2013; 28 (1): 488-497. doi: 10.1109/TPEL.2012.2195203.
- [14] Vindel D, Haghbin S, Rabiei A, Carlson O, Ghorbani R. Field-oriented control of a PMSM drive system using the dSPACE controller. IEEE International Electric Vehicle Conference, Greenville, SC; 2012. pp. 1-5. doi: 10.1109/IEVC.2012.6183206.
- [15] Nam K. Sensorless control of IPMSM. In: Handbook of AC motor control and electric vehicle applications, New York, NY, USA: CRC Press, 2010, pp. 229-268.

- [16] Cortes P, Kazmierkowski MP, Kennel RM, Quevedo DE, Rodriguez J. Predictive control in power electronics and drives. *IEEE Transactions on Industrial Electronics* 2008; 55 (12): 4312-4324. doi: 10.1109/TIE.2008.2007480
- [17] Fuentes EJ, Silva CA, Yuz JI. Predictive speed control of a two-mass system driven by a permanent magnet synchronous motor. *IEEE Transactions on Industrial Electronics* 2012; 59(7): 2840-2848. doi: 10.1109/TIE.2011.2158767
- [18] Usama M, Jaehong K. Vector control algorithm based on different current control switching techniques for ac motor drives. *E3S Web of Conferences* 2020; 152: 03009. doi.org/10.1051/e3sconf/202015203009
- [19] Bolognani S, Bolognani S, Pereti L, Zigliotto M. Design and implementation of model predictive control for electrical motor drives. *IEEE Transaction on Industrial Electronic* 2009; 56 (6): 1925-1936. doi:10.1109/TIE.2008.2007547
- [20] Hammoud I, Hentzelt S, Oehlschlaegel T, Kennel R. Computationally efficient finite-set model predictive current control of interior permanent magnet synchronous motors with model-based online inductance estimation. *2019 IEEE Conference on Power Electronics and Renewable Energy* 2019; 290-295, doi: 10.1109/CPERE45374.2019.8980058.
- [21] Vazquez S, Aguilera RP, Pablo JP, Agelidis VG. Model predictive control for single-phase npc converters based on optimal switching sequences. *IEEE Transaction on Industrial Electronic* 2016; 63: 7533-7541. doi:10.1109/TIE.2016.2594227
- [22] Kakosimos P, Abu-Rub H. Predictive Speed Control with Short Prediction Horizon for Permanent Magnet Synchronous Motor Drives. *IEEE Transaction Power Electronics* 2018; 33: 2740–2750.
- [23] Preindl M, Bolognani S. Model predictive direct speed control with finite control set of PMSM drive systems. *IEEE Transactions on Power Electronics* 2013; 28(2): 1007-1015. doi: 10.1109/TPEL.2012.2204277
- [24] Zhang Y, Huang L, Xu D, Liu J, Jin J. Performance evaluation of two-vector-based model predictive current control of PMSM drives. *Chinese Journal Electrical Engineering* 2018; 4: 65-81.
- [25] Nam K. Rotating Field Theory. *Handbook of AC motor control and electric vehicle applications*. New York: CRC Press, 2010 pp. 33-51.
- [26] Amornwongpeeti S, Kiselychuk O, Wang J, Shah N, Soumelidis M. Speed control of IPMSM motor drives using model reference adaptive technique. *2017 International Conference on Applied System Innovation (ICASI)*, Sapporo; 2017. pp. 672-675. doi: 10.1109/ICASI.2017.7988515
- [27] Li Z, L Hi. MTPA control of PMSM system considering saturation and cross-coupling. 2012. In: *15th International Conference on Electrical Machines and Systems (ICEMS)*; Sapporo, Japan; 2012. pp. 1-5.
- [28] Garin. S, and Nasir UM. Harmonic Injection-based adaptive control of IPMSM motor drive for reduced motor current THD. *IEEE Transactions on Industry Applications* 2017; 53 (1): 483-491. doi: 10.1109/TIA.2016.2603145
- [29] Gmati B, El Khil S, Slama-Belkhodja I. Improved MPC for PMSM drives to reduce switching losses. *2017 International Conference on Green Energy Conversion Systems (GECS)*, Hammame, pp.1-8.
- [30] Akter, MP et al. Stability and performance investigations of model predictive controlled active-front-end (AFE) rectifiers for energy storage systems. *Journal of Power Electronics* 2015; 15 (1): pp. 202-215. doi: 10.6113/JPE.2015.15.1.202.
- [31] Rodriguez J, Cortes P. Predictive control of a three-phase inverter. In: *Handbook of Predictive Control of Power Converter and Electrical Drives*, United Kingdom: Wiley-IEEE Press, 2012, pp. 43-63.
- [32] Palais RS, Palais RA. *Differential equations, mechanics, and computation*. USA: American Mathematical Society, 2009.
- [33] Usama M, Jaehong K. Simplified model predicted current control method for speed control of non-silent permanent magnet synchronous motors. In: *3rd International Conference on Computing, Mathematics and Engineering Technologies (iCoMET)*, Sukkur, Pakistan; 2020. pp. 1-5. doi: 10.1109/iCoMET48670.2020.9073884

- [34] Nam K. Pulse-Width Modulation and Inverter. In: Handbook of AC Motor Control and Electric Vehicle Applications, New York, NY, USA: CRC Press, 2010, pp. 269-293.
- [35] Zhang Y, Xu D, Liu J, Gao S, Xu W. Performance improvement of model-predictive current control of permanent magnet synchronous motor drives. IEEE Transactions on Industry Applications 2017; 53(4): 3683-3695.